

Supplementary Information

Light-activated semiconducting polymer dots as mimic oxidases with remarkable catalytic efficiency: characteristics, mechanisms, and applications

Xueli Chen, Junyong Sun*, Qiang Zhang, Xuekai Jiang, and Feng Gao*

Laboratory of Functionalized Molecular Solids, Ministry of Education, Anhui Key Laboratory of Chemo/Biosensing, Laboratory of Biosensing and Bioimaging (LOBAB), College of Chemistry and Materials Science, Anhui Normal University, Wuhu 241002, P. R. China

*Corresponding author. Phone/Fax: +86-553-3937137.

E-mail: fgao@mail.ahnu.edu.cn, sunjy228@mail.ahnu.edu.cn

Contents

1. Experimental Section	S2
1.1 Reagents	S2
1.2 Preparation of different Pdots	S2
1.3 Characterization of Pdots.	S3
1.4 The effect of excitation wavelength and power density on catalytic activity	S3
1.5 Evaluation of oxidase-like activity of Pdots	S4
1.6 Measurement of AChE activity	S4
2. Supplementary Figures	S5
Fig. S1. Investigation of the oxidation reaction of ABTS and OPD using light-activated PFO Pdots as oxidase mimics.	S5
Fig. S2. Effects of excitation wavelength and power density on the catalytic activity of PFO Pdots	S5
Fig. S3. Optimization of experimental conditions for oxidase-like activity of PFO Pdots.	S6
Fig. S4. Comparison of catalytic performances of Pdots with Ag ⁺ and Fe ³⁺	S6
Fig. S5. Determination of kinetic parameters of Pdots as oxidase mimics.....	S7
Fig. S6. Investigation of the catalytic performances of Pdots with different sizes and surface charges.....	S7
Fig. S7. Investigation of the catalytic performances of Pdots prepared from different polymers.	S8
Fig. S8. UV-Vis and fluorescence spectra of PFO / PFDBT-5 Pdots.....	S8
Fig. S9. Studies on the mechanisms of PFO / PFDBT-5 Pdots for AChE detection	S9

Fig. S10. Condition optimization for detecting AChE.	S9
Fig. S11. The selectivity of PFO / PFDBT-5 Pdots probe for AChE detection.....	S10
Fig. S12 Fluorescence spectra of the sensing system at various AChE concentrations and the corresponding visual photographs.	S10
Fig. S12. Visual detection of AChE activity.	S11
3. Supplementary Tables	S11
Table S1. Comparison of kinetic parameters of different oxidase mimics.	S11
Table S2. Comparison of analytical performances for AChE detection with different methods.	S12
4. Supplementary References	S12

1. Experimental Section

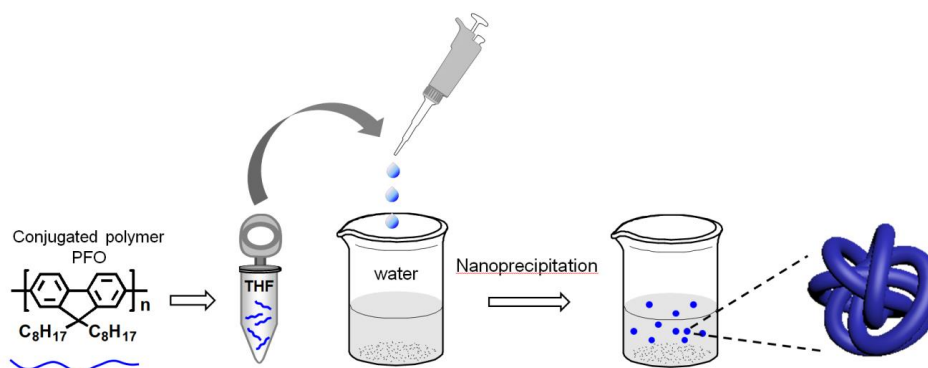
1.1 Reagents

All chemicals used in this work are of analytical grade and used as received without further purification. Poly(9,9-dioctylfluorenyl-2,7-diyl)-end-capped with dimethylphenyl (PFO; average MW, 89000; polydispersity, 2.3), poly[2-methoxy-5-(2-ethylhexyloxy)-1,4-phenylenevinylene] (MEH-PPV, MW 200 000, polydispersity 4.0), poly[2-methoxy-5-(2-ethylhexyloxy)-1,4-(1-cyanovinylene-1,4-phenylene)] (CN-PPV, average MW 353,000, polydispersity 9.4) and poly[(9,9-dioctylfluorenyl-2,7-diyl)-co-(1,4-benzo-{2,1',3}-thiadiazole)] (PFBT, MW 164 000, polydispersity 3.4) were procured from ADS Dyes, Inc. (Quebec, Canada). Poly(9,9-dioctylfluorene)-co-(4,7-di-2-thienyl-2,1,3-benzothiadiazole) (PFDBT-5) was donated by Prof. Changfeng Wu from South University of Science and Technology of China. Acetylcholinesterase (AChE), acetylthiocholine (ATCh), 2,2'-azinobis-(3-ethylbenzthiazoline-6-sulphonate) (ABTS), o-phenyldiamine(OPD), superoxide dismutase (SOD), 9,9-Di-n-octylfluorene (FO), tetrahydrofuran (THF, anhydrous, $\geq 99.9\%$, inhibitor-free), and 3,3',5,5'-tetramethylbenzidine (TMB) were purchased from Sigma-Aldrich. Deionized water with a resistivity greater than 18.25 M Ω cm was used in all of the experiments.

1.2 Preparation of different Pdots

The Pdots were prepared via classical nanoprecipitation (Scheme 1) according to the previous reports.^{1,2} In brief, different polymers are dissolved in anhydrous THF to obtain 1.0 mg mL⁻¹ stock solutions under vigorous sonication, respectively. A 3 mL THF homogeneous solution containing 50 μ g mL⁻¹ of stock solution is injected into

10 mL of ultrapure water in a vigorous bath sonicator. After sonication for 5 min, the THF is removed by nitrogen stripping and the solution is concentrated by continuous nitrogen stripping to 3 mL on a 95°C hot plate. Afterward, the solution is filtered through a 0.22 μm filter membrane to remove any aggregation particles and precipitations.



Scheme 1. Schematic of classical nanoprecipitation for Pdots preparation

The PFO/PF-DBT5 Pdots are prepared according to our previous work with some modifications³. Typically, the conjugated polymer PFO and PF-DBT5 are separately dissolved in tetrahydrofuran (THF) to prepare a 1.0 mg mL⁻¹ solution, respectively. A 3 mL THF homogeneous solution containing 32 $\mu\text{g mL}^{-1}$ PFO and 18 $\mu\text{g mL}^{-1}$ PFDBT-5 are injected into 10 mL of ultrapure water in a vigorous bath sonicator. The following preparation procedures are same as mentioned above.

1.3 Characterization of Pdots

The fluorescence and UV-vis absorption spectrum was recorded on a LS-55 spectrophotometer (PerkinElmer, USA) and a Lambda-35 UV-Vis spectrophotometer (PerkinElmer, USA), respectively. Luminescence lifetime and quantum yield measurements were carried out on a FLS 1000 spectrofluorometer (Edinburgh Instruments, UK). The morphology of Pdots was characterized with a HT-7700 transmission electron microscope (Hitachi, Japan) operating at an accelerating voltage of 100 kV. For TEM, a 7 μL Pdots aqueous solution (diluted 10-fold) was placed on a carbon-coated grid and the water was evaporated at room temperature. A ZS90 Zetasizer Nano instrument (Malvern, UK) was used to measure the hydrodynamic size and zeta potential. For DLS and Zeta potential determination, Pdots aqueous solution (diluted 10-fold, 0.22 micron filter) was taken in cell and tested in parallel on a ZS90 Zetasizer Nano instrument three times (dispersant: water; temperature: 25 $^{\circ}\text{C}$; equilibration time: 120s).

1. 4 The effects of excitation wavelength and power density on catalytic activity of Pdots

In this experiment, a multi-color (white, purple, blue and yellow) light-emitting diode (LED) lamps (30 W), which can emits strong (30 W), middle (15 W) or weak (7.5 W) three gears power light through the power control switch, is employed for the irradiation source. In the dark conditions, the solution containing 0.25M TMB, 2 μ g/mL PFO Pdots and 0.2M NaAc-HAc was irradiated with white, purple, blue and yellow light at 30 W power level for 1 h, respectively. Then the absorbance at 652 nm was measured to study the effect of excitation wavelength. For another control experiment, similar operations were carried out except that the white light with different power density (30 W, 15W and 7.5 W) was employed as the irradiation source.

1.5 Evaluation of oxidase-like activity of Pdots

For mimic oxidase studies, TMB was chosen as a colorimetric substrate. Steady-state kinetic assays were carried out in 96-well plate using PFO Pdots (2 μ g mL⁻¹) at room temperature with different concentrations of TMB in 0.2 M NaAc-HAc buffer of pH 4.0. Reactions were monitored at 652 nm for TMB in time-course mode using a microtiter plate reader.

1. 6 Measurement of AChE activity

In series of 600 μ L colorimetric tubes, 5 μ L of 10 mM ATCh and different amount of AChE were added, and incubated for 30 min at 37 $^{\circ}$ C. After reaction, 10 μ L of 0.25 mM TMB and 10 μ L of 50 μ g mL⁻¹ PFO/PFDBT-5 Pdots were added into the above solution. The final volume of reaction system was adjusted to 200 μ L with NaAc-HAc buffer solution (0.2 M, pH 4.0). With another reaction for 120 min at 45 $^{\circ}$ C, the fluorescence spectra were measured with excitation of 380 nm.

2. Supplementary Figures

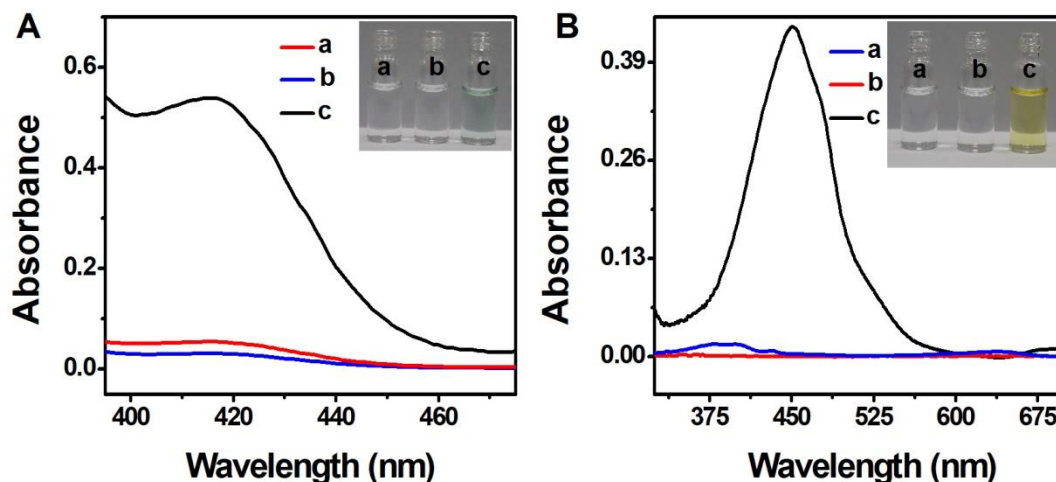


Fig. S1. (A) UV-Vis spectra and the corresponding photographs of different reaction systems of 0.25 mM ABTS under natural light (a), 0.25 mM ABTS + 2 μg mL⁻¹ Pdots shielded from light (b), and 0.25 mM ABTS + 2 μg mL⁻¹ Pdots under natural light (c) in 0.2 M, pH 4.0 acetic acid-acetate buffer incubated for 120 min at 45 °C. (B) UV-Vis spectra and the corresponding photographs of different reaction systems of 0.25 mM OPD under natural light (a), 0.25 mM OPD + 2 μg mL⁻¹ Pdots shielded from light (b), and 0.25 mM OPD + 2 μg mL⁻¹ Pdots under natural light (c) in 0.2 M, pH 4.0 acetic acid-acetate buffer for 120 min at 45 °C.

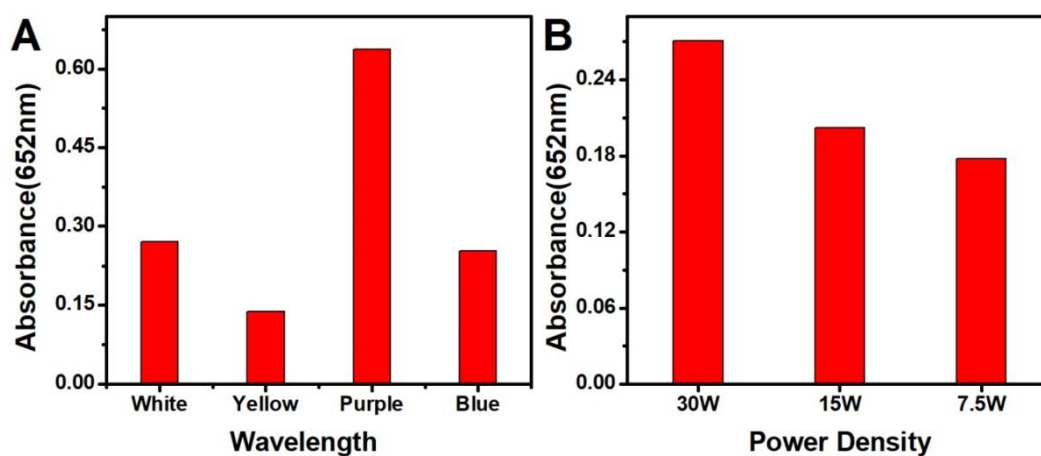


Fig. S2. The influence of excitation wavelength (A) and power density (B) on the oxidation of 0.25 mM TMB by 2 μg mL⁻¹ PFO Pdots in 0.2 M, pH 4.0 acetic

acid-acetate buffer.

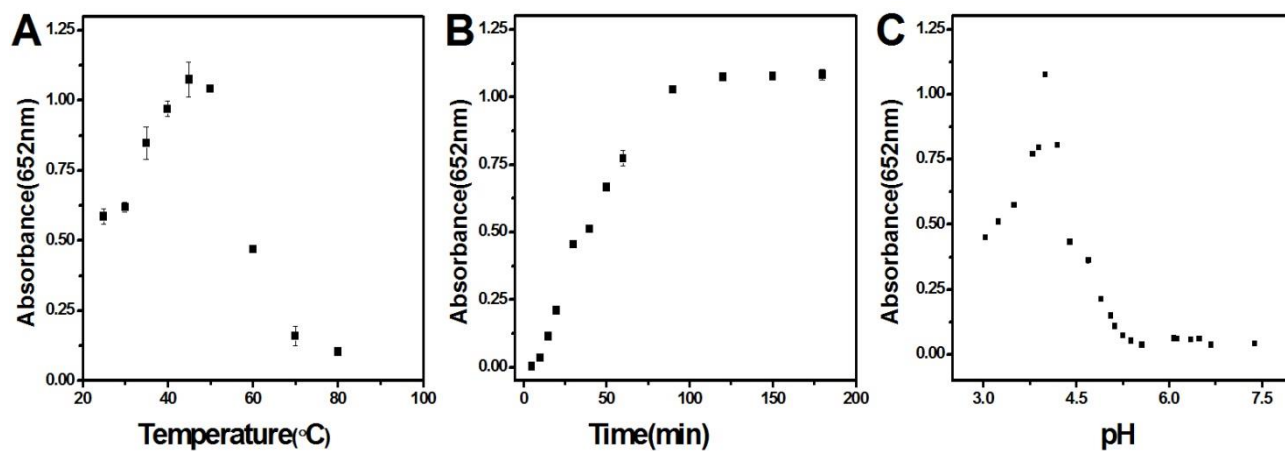


Fig. S3. The effect of temperature (A), time (B) and pH (C) on the oxidation of 0.25 mM TMB by $2 \mu\text{g mL}^{-1}$ PFO Pdots in 0.2 M, pH 4.0 acetic acid-acetate buffer.

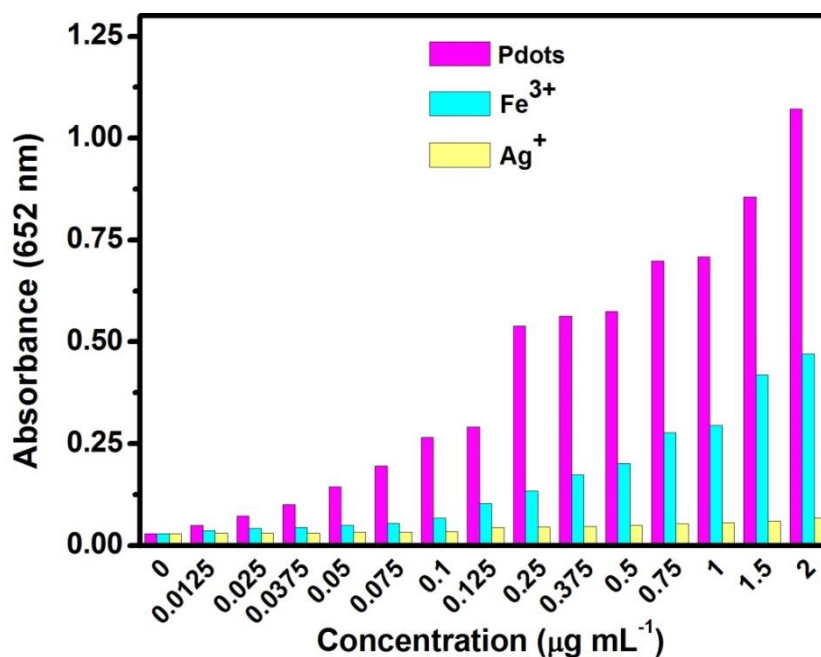


Fig. S4. Comparison of the absorbance at 652 nm of 0.25 mM TMB in the presence of different concentrations of PFO Pdots, Ag^+ and Fe^{3+} in 0.2 M, pH 4 NaAc-HAc buffer. The reaction temperature and reaction time are 45°C , 120 min, respectively.

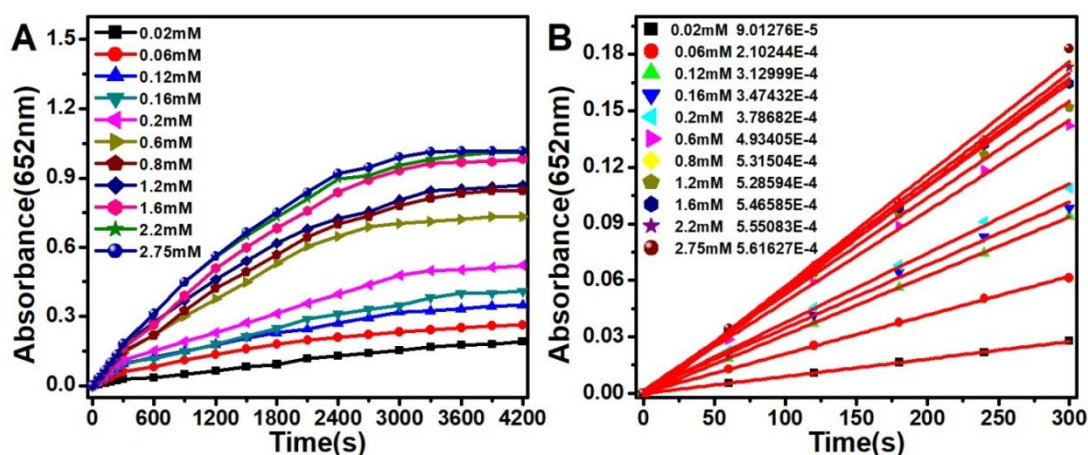


Fig. S5. (A) Time-dependent absorption spectra of TMB with different concentrations in 0.2M, pH 4 NaAC-HAC buffer solution in the presence of $2 \mu\text{g mL}^{-1}$ PFO Pdots. (B) Linear fitting curve of corresponding initial velocity (recation time: 300s). The incubation temperature is $45 \text{ }^\circ\text{C}$.

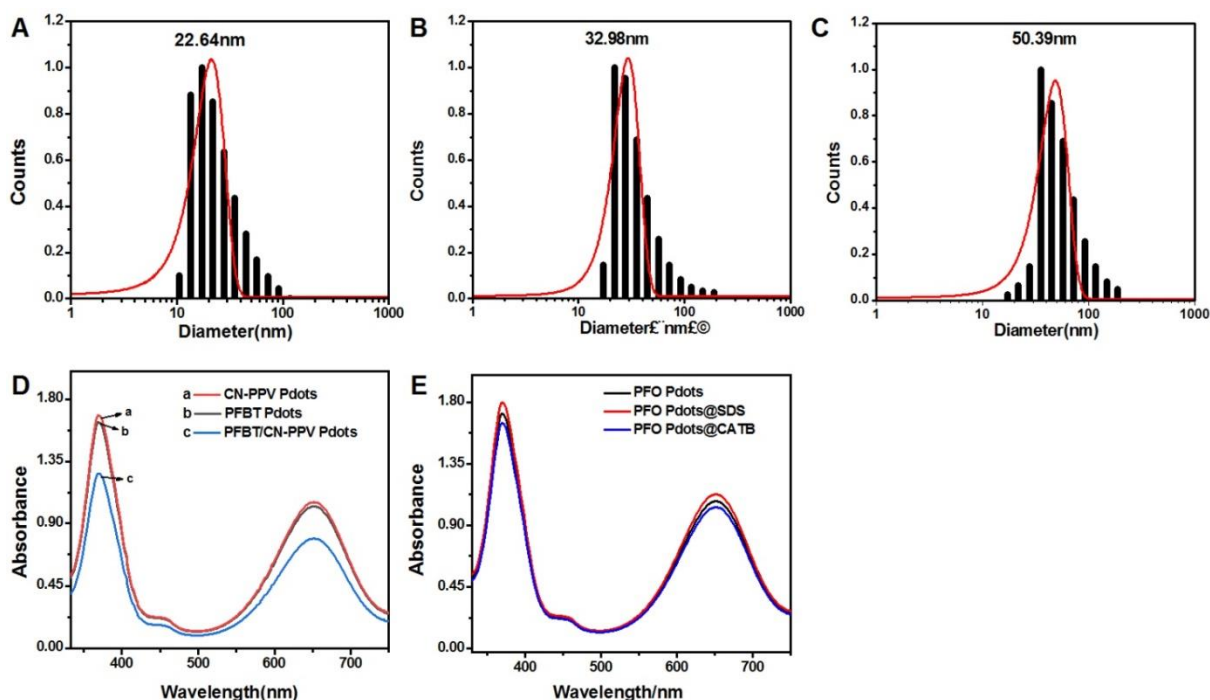


Fig. S6. (A, B, C) Dynamic light scattering measurements of PFO Pdots with different sizes. (D) The UV-Vis spectra of TMB system by using single component CN-PPV (curve a), PFBT (curve b) Pdots and PFBT/CN-PPV hybrid Pdots (curve c) as mimic oxidase, respectively. (E) UV/vis spectrum of TMB (0.25 mM) in acetic acid buffer solution (0.2 M , $\text{pH } 4.0$) containing PFO Pdots ($2 \mu\text{g mL}^{-1}$) with different surface potentials incubated for 120 min at $45 \text{ }^\circ\text{C}$.

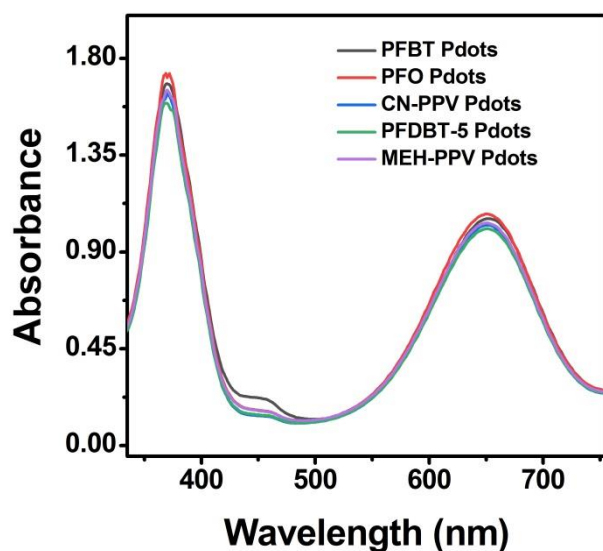


Fig. S7. UV-Vis spectra of 0.25 mM TMB in 0.2 M, pH 4.0 acetic acid buffer solution containing $2 \mu\text{g mL}^{-1}$ Pdots prepared from different polymer incubated for 120 min at 45 °C.

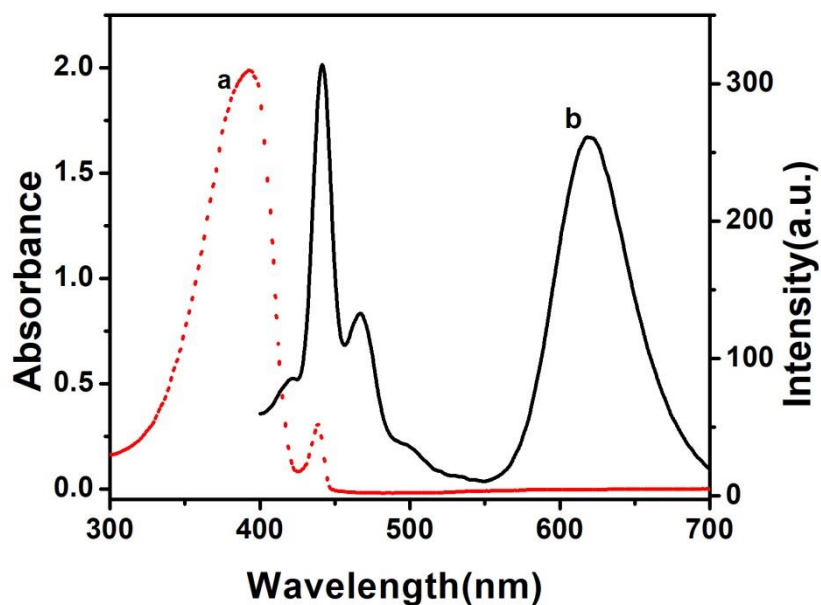


Fig. S8. UV-Vis (a) and fluorescence (b) spectrum of PFO/PFDBT-5 Pdots in water.

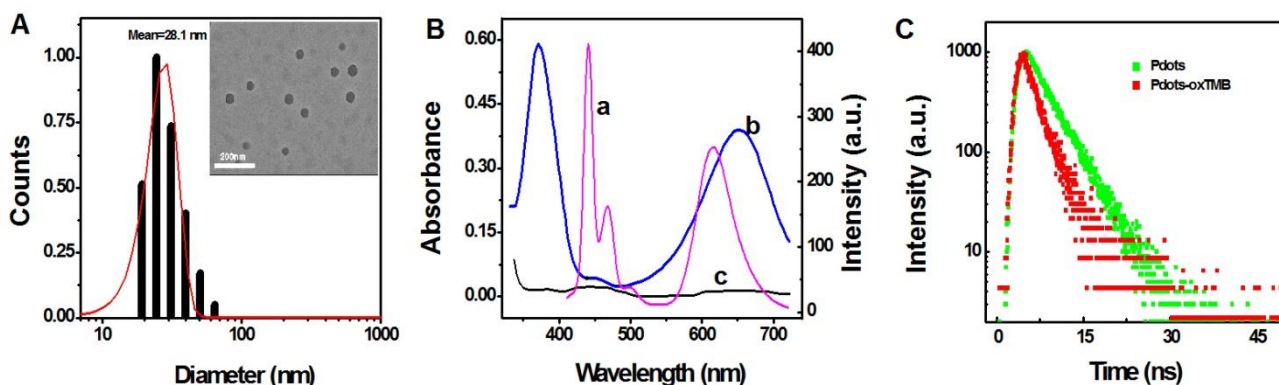


Fig. S9. (A) Dynamic light scattering measurements of PFO/PFDBT-5 Pdts. Inset: Transmission electron microscopy of PFO/PFDBT-5 Pdts. (B) The spectra overlaps of different emission bands of PFO/PFDBT-5 Pdts (curve a) and absorption spectra of TMB (curve c) and TMB_{ox} (curve b). (C) Time-resolved fluorescence spectra of PFO/PFDBT-5 Pdts (green dot) and PFO/PFDBT-5 Pdts-TMB_{ox} system (red dot) at 619 nm.

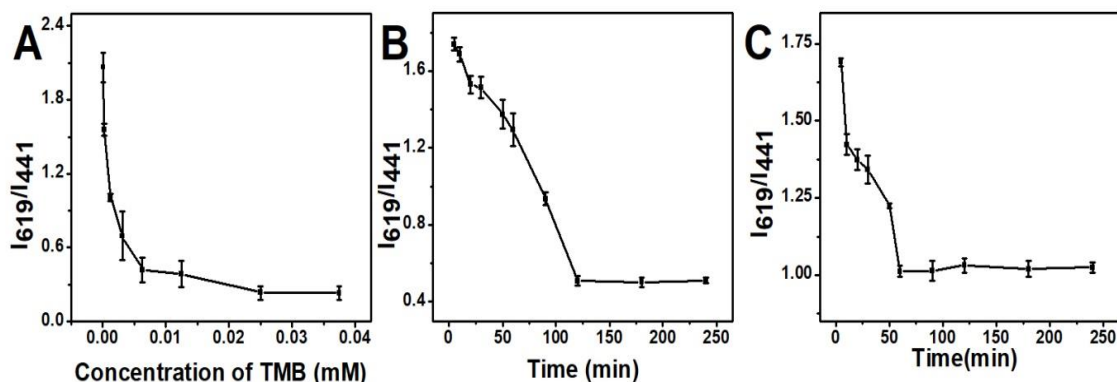


Fig. S10. (A) The effect of TMB concentration on the Pdts-based probe for AChE detection. (B) The effect of incubation time on the Pdts-based probe for AChE detection (0.0125 mM TMB, 0.25 mM ATCh). (C) The effect of incubation time on the Pdts-based probe for AChE detection (0.0125 mM TMB, 0.25 mM ATCh and 500 U L⁻¹ AChE). The conditions for three experiments are: 2.5 $\mu\text{g mL}^{-1}$ PFO/PFDBT-5 dots, 0.2M, pH4 NaAc-HAc buffer, reaction temperature 45 $^{\circ}\text{C}$.

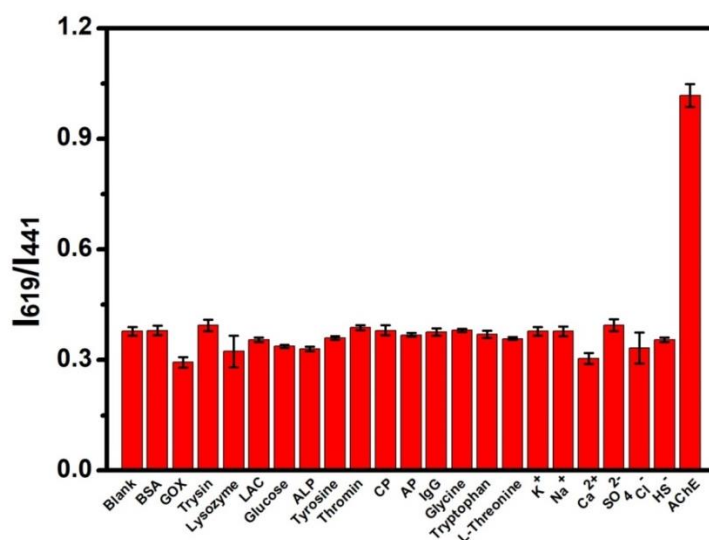


Fig. S11 The relative fluorescence intensity (I_{619}/I_{441}) of different species in the proposed Pdots-TMB sensing system. The species include BSA (0.25 g mL^{-1}), GOx (5 U mL^{-1}), trysin (5 U mL^{-1}), lysozyme (5 U mL^{-1}), LAC (5 U mL^{-1}), glucose (0.25 g mL^{-1}), ALP (5 U mL^{-1}), tyrosine (5 U mL^{-1}), thrombin (5 U mL^{-1}), carboxypeptidase (5 U mL^{-1}), aminopeptidase (5 U mL^{-1}), immunoglobulin G (0.25 g mL^{-1}), glycine (0.25 g mL^{-1}), tryptophan (0.25 g mL^{-1}), L-threonine (0.25 g mL^{-1}), K^+ (0.25 g mL^{-1}), Na^+ (0.25 g mL^{-1}), Ca^{2+} (0.25 g mL^{-1}), SO_4^{2-} (0.25 g mL^{-1}), Cl^- (0.25 g mL^{-1}), HS^- (0.25 g mL^{-1}) and AChE (0.5 U mL^{-1}). Reaction conditions: 0.2 M , $\text{pH } 4.0$ NaAc-HAc buffer, PFO/PFDBT-5 Pdots $2.5 \mu\text{g mL}^{-1}$, TMB 0.0125 mM , ATCh 0.25 mM , incubation time 120 min . Error bars illustrate the standard deviations of three independent measurements.

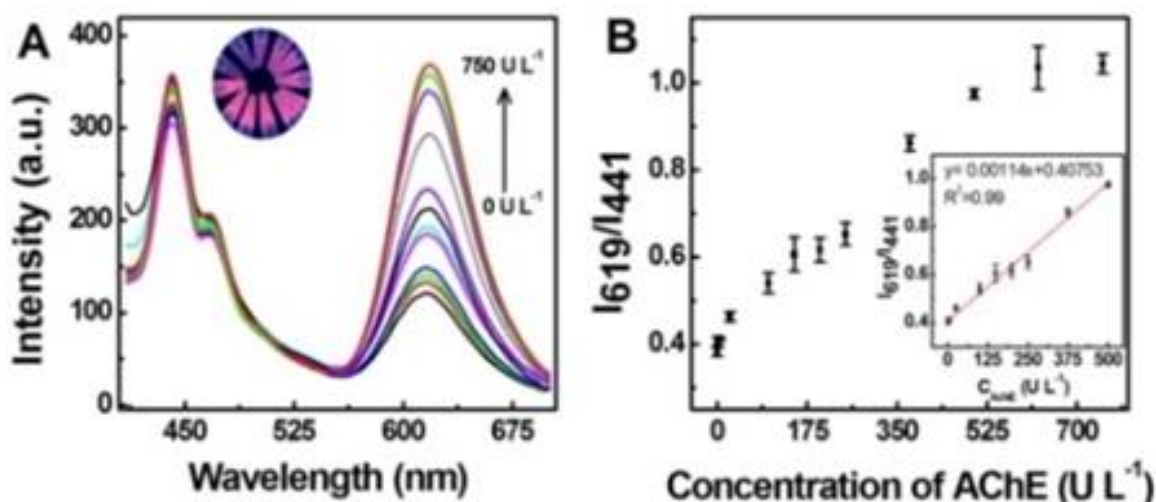


Fig. S12 Fluorescence spectra of the sensing system at various AChE concentrations and the corresponding visual photographs under 365 nm UV light (inset). (B) Plot of intensity ratio (I_{619}/I_{441}) against AChE concentration and the linear regression curve (inset).

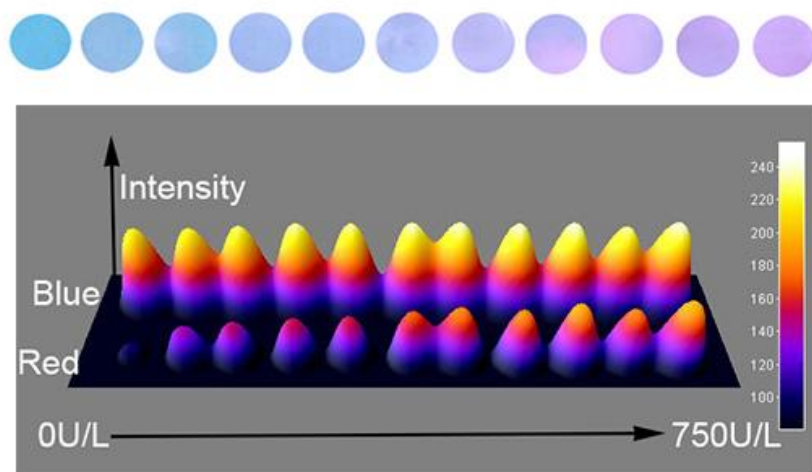


Fig. S13 PFO/PFDBT-5 Pdots-based test strips for visual detection of AChE activity. The concentrations of AChE (from left to right side) are 0, 1.25, 5, 25, 100, 150, 200, 250, 400, 500, 750 U L⁻¹, respectively.

3. Supplementary Tables

Table S1. Comparison of kinetic parameters of different oxidase mimics.

Materials	K_m /mM	V_{max} /mM s ⁻¹	K_{cat}	K_{cat}/K_m	Ref
porous manganese oxide/manganese ferrite nanopopcorns	0.128	2.58×10^{-5}	5.16×10^{-4} / $\mu\text{Ms}^{-1} \mu\text{g}^{-1} \text{mL}$	4.02×10^{-6} / $\text{s}^{-1} \mu\text{g}^{-1} \text{mL}$	4
photosensitized metal-organic framework	0.165	1.39×10^{-4}	2.317×10^{-3} / $\mu\text{Ms}^{-1} \mu\text{g}^{-1} \text{mL}$	1.404×10^{-5} / $\text{s}^{-1} \mu\text{g}^{-1} \text{mL}$	5
selenium nanoparticles	8.3	5.07×10^{-5}	8.45×10^{-4} / $\mu\text{Ms}^{-1} \mu\text{g}^{-1} \text{mL}$	1.018×10^{-7} / $\text{s}^{-1} \mu\text{g}^{-1} \text{mL}$	6
fluorescein	0.158	6.717×10^{-15}	6.717×10^{-2} / s^{-1}	4.25×10^2 / $\text{mM}^{-1} \text{s}^{-1}$	7
Fe-N-C artificial enzyme	4.58	1.39×10^{-4}	5.56×10^{-3} / $\mu\text{Ms}^{-1} \mu\text{g}^{-1} \text{mL}$	1.2139×10^{-6} / $\text{s}^{-1} \mu\text{g}^{-1} \text{mL}$	8
nanoceria coated with poly(acrylic acid)	3.8	7×10^{-4}	0.14 / s^{-1}	3.68×10^{-2} / $\text{mM}^{-1} \text{s}^{-1}$	9
PFO Pdots	0.106	1.497×10^{-5}	6.84485×10^6 / s^{-1}	6.426×10^7 / $\text{mM}^{-1} \text{s}^{-1}$	This work
			7.485×10^{-3} / $\mu\text{Ms}^{-1} \mu\text{g}^{-1} \text{mL}$	7.06132×10^{-5} / $\text{s}^{-1} \mu\text{g}^{-1} \text{mL}$	

Table S2. Comparison of Analytical Performances for AChE detection with different methods.

Probe	Linear range / μL^{-1}	Detection limit / μL^{-1}	Sensing type	Ref.
MoOx quantum dots	5.0-150	5.0	photoluminescence, off-on-off	10
GODs-MnO ₂	1-200	0.37	fluorimetry, turn-on	11
AuNPs	-	0.6	colorimetry	12
PEI-CuNCs	3.0–200	1.38	fluorimetry, off-on-off	13
carbon quantum dots	14.2- 121.8	4.25	fluorimetry, on-off-on	14
3-mercaptopropionic acid stabilized QDs	100-2500	20	fluorimetry, turn-on	15
PFO/PFDBT-5 Pdots	0-500	0.59	fluorimetry, ratiometric	This work

4. Supplementary References

- (1) S. Y. Kuo, H. H. Li, P. J. Wu, C. P. Chen, Y. C. Huang and Y. H. Chan, *Anal. Chem.*, 2015, **87**, 4765-4771.
- (2) K. Sun, Y. Yang, H. Zhou, S. Yin, W. Qin, J. Yu, D. T. Chiu, Z. Yuan, X. Zhang and C. Wu, *ACS Nano*, 2018, **12**, 5176-5184.
- (3) J. Sun, P. Ling and F. Gao, *Anal. Chem.*, 2017, **89**, 11703-11710.
- (4) C. W. Wu, B. Unnikrishnan, Y. T. Tseng, S. C. Wei, H. T. Chang and C. C. Huang, *J. Colloid Interface Sci.*, 2019, **541**, 75-85.
- (5) Y. F. Liu, M. Zhou, W. Cao, X. Y. Wang, Q. Wang, S. R. Li and H. Wei, *Anal. Chem.*, 2019, **91**, 8170-8175.
- (6) L. Guo, K. Huang and H. Liu, *J. Nanopart. Res.*, 2016, **18**, 74.
- (7) L. Liu, C. Sun, J. Yang, Y. Shi, Y. Long and H. Zheng, *Chem. Eur. J.*, 2018, **24**, 6148-6154.
- (8) F. He, L. Mi, Y. Shen, T. Mori, S. Liu and Y. Zhang, *ACS Appl. Mater. Interfaces*, 2018, **10**, 35327-35333.
- (9) A. Asati, S. Santra, C. Kaittanis, S. Nath and J. M. Perez, *Angew. Chem. Int. Ed.*, 2009, **48**, 2308-2312.
- (10) S. J. Xiao, Z. J. Chu, X. J. Zhao, Z. B. Zhang and Y. H. Liu, *Microchim. Acta*, 2017, **184**, 4853-4860.

- (11) J. Deng, D. Lu, X. Zhang, G. Shi and T. Zhou, *Environ. Pollut.*, 2017, **224**, 436-444.
- (12) M. Wang, X. Gu, G. Zhang, D. Zhang and D. Zhu, *Langmuir*, 2009, **25**, 2504-2507.
- (13) J. Yang, N. Song, X. Lv and Q. Jia, *Sens. Actuators, B*, 2018, **259**, 226-232.
- (14) Z. Qian, L. Chai, C. Tang, Y. Huang, J. Chen and H. Feng, *Sens. Actuators, B*, 2016, **222**, 879-886.
- (15) Z. Chen, X. Ren and F. Tang, *Chin. Sci. Bull.*, 2013, **58**, 2622-2627.